Solar Flares and Magnetospheric Particles: Investigations Based Upon the ONR-602 and ONR-604 Experiments

Performance Report

ONR Grant

N00014-90-J-1466

Second Quarter FY93

John P. Wefel and T. Gregory Guzik

Department of Physics and Astronomy
Louisiana State University
Baton Rouge, LA 70803-4001

Phone: 504-388-8696
FAX: 504-388-1222

3 May 1993

"Solar Flares and Magnetospheric Particles: Investigations Based Upon the ONR-602 and ONR-604 Experiments"

I. Introduction:

This performance report covers work accomplished under ONR Grant N00014-90-J-1466 related to the radiation environment in near-Earth space. The goal of the research is to measure and describe, quantitatively, the Geospace radiation environment in which men and spacecraft must survive and function. The tools for this investigation are the data returned by the ONR-602 and ONR-604 experiments, both flown under the auspices of ONR and the Air Force Space Test Program, augmented by correlative databases of both space-based and ground-based data. The investigation involves data analysis, modeling and applications to a variety of space equipment and environments.

This report builds upon the detailed Technical Report (Fall, 1992) and the previous performance report. For the current period, the principal effort was in the analysis of the solar energetic particle events that occurred during the CRRES mission, focusing upon the helium component.

II. Solar Energetic Particle (SEP) Analysis:

CRRES was launched into a period of strong solar activity. Figure 1 shows a plot of the "cleaned" helium counting rate over the full mission. At least 26 separate SEP events can be identified from Figure 1, a dozen of which have been selected for detailed analysis. Of these twelve, listed in Table 1, the largest are the March and June 1991 periods for which we have previously reported preliminary results.

A. Background Rejection:

The data in Figure 1 are the result of background removal from the raw data returned by the ONR-604 instrument. A particle is identified as a good helium candidate if it enters the experiment from the top, deposits enough energy in at least one of the 5 mm detectors (K*i*, i=1,...,8) to trigger the medium level discriminator (~37 MeV) and stops in the K*i* detector stack. Accordingly, each incident particle should pass the following three criteria to qualify: (1) the range ID (the identification number of the stopping detector) is greater than or equal to 7 (stopping in K1) and is less than or equal to 14 (stoping in K8); (2) the scintillator discriminator is not triggered; and (3) the radius of the incidence point in the stopping detector is less than 18.75 mm (radius of the K*i* detectors).

The most important step in the analysis is to utilize the observed energy deposited in each detector (i.e., more information than just employing the last two detectors) to make an overall consistency check between calculated and observed energies, which serves as a powerful tool to discriminate good helium from heavier ions and low-Z background, and provides an accurate and reliable charge and mass for each incident particle. A parameter DE is introduced for this purpose:

$$DE = \sqrt{\sum_i [Ecal(i) - Eobs(i)]^2} / Eobs, \qquad (1)$$

where Ecal(i) and Eobs(i) are the calculated and the observed energies deposited in the ith detector, respectively, and

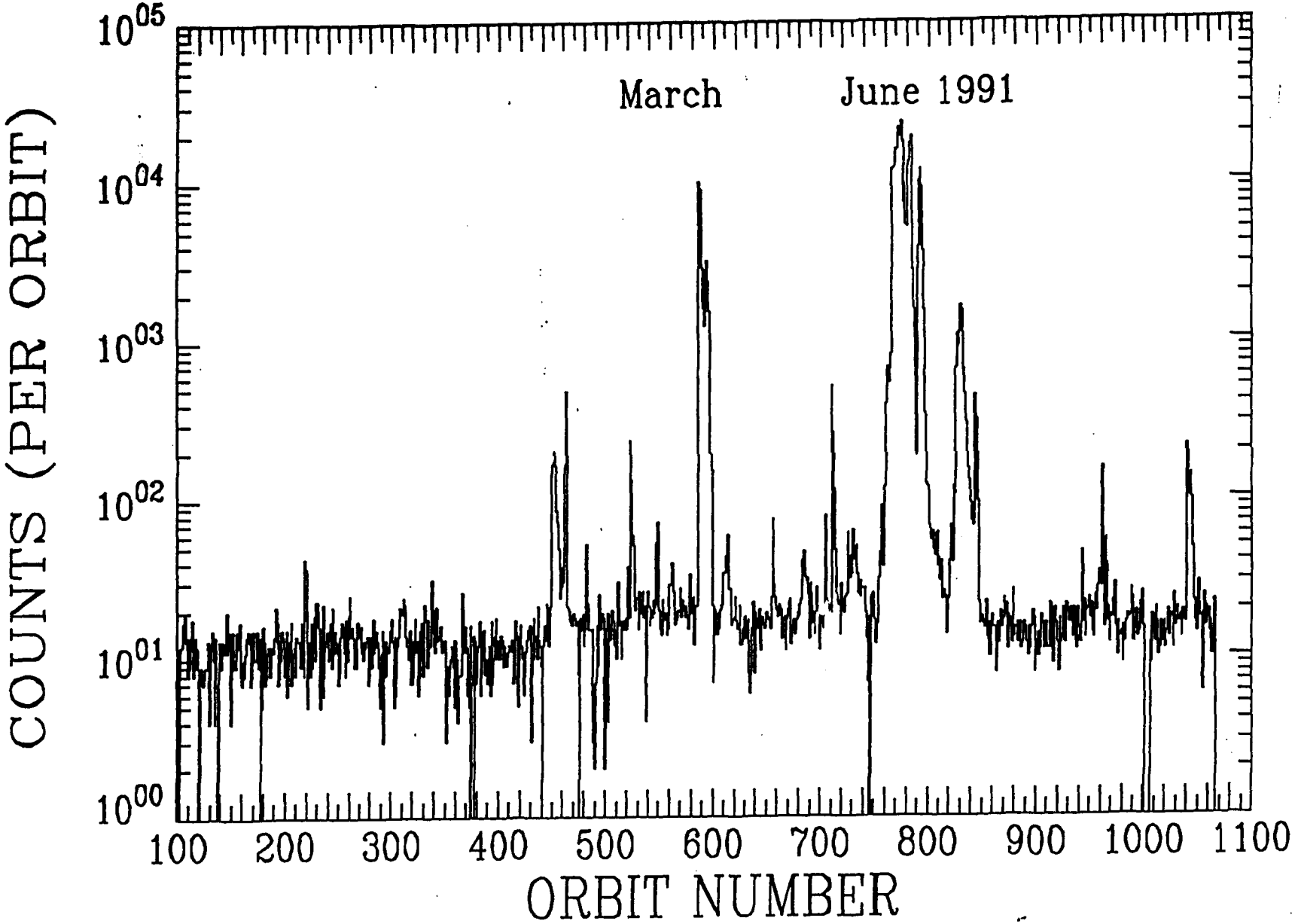

Figure 1. Helium intensity (counts per orbit) observed during the CRRES mission.

TABLE 1. Major SEP Events During the CRRES Mission

Event Number	Peak Orbit	Start (Day)	Peak (Day)	End (Day)	Peak He (cnt/orb)	P1/He (10^{-4})	Assoc. Flare (Day/UT)
1	451	26.0	27.2	29.3	201	-	Jan 25/0630
2	462	31.3	31.7	32.4	481	-	Jan 31/0230
3	522	56.4	56.5	57.6	235	-	Feb 25/0819
4	586	82.1	82.6	84.0	10000	9±2	Mar 22/2247
5	593	84.6	85.4	87.6	3234	-	Mar 24/2046
6	710	133.1	133.4	135.0	517	-	May 13/0144
7	774	153.0	159.6	162.1	23404	1.7±0.5	Jun 04/0352
8	783	162.1	163.4	165.5	19135	2.9±0.7	Jun 11/0209
9	792	166.3	167.2	173.6	11918	10±2	Jun 15/0821
10	829	179.5	183.0	188.3	1648	-	Jun 28/0626
11	842	188.4	188.6	190.3	450	-	Jul 07/0223
12	961	238.7	239.7	241.4	156	-	Aug 25/0115

TABLE 2. Average Helium Spectra and Correction Factor

Event Number	Amplitude A^*	Index γ	c	Fluence** (at E_0)	Duration (Days)
1	0.165±0.015	2.09±0.45	1.2158	4.7×10^{4}	3.3
2	0.161±0.017	5.10±0.53	1.9993	1.5×10^{4}	1.1
3	0.120±0.004	1.44±0.21	1.0952	1.2×10^{4}	1.2
4	9.14±0.40	6.80±0.22	2.6618	2.0×10^{6}	2.5
5	1.030±0.025	5.13±0.12	2.0119	2.7×10^{5}	3.0
6	0.221±0.012	3.20±0.45	1.4603	3.6×10^{4}	1.9
7	9.56±0.33	4.31±0.17	1.7550	7.5×10^{6}	9.1
8	36.14±0.53	4.26±0.08	1.7398	1.1×10^{7}	3.4
9	3.98±0.09	4.04±0.11	1.6756	2.5×10^{6}	7.3
10	0.385±0.007	4.48±0.08	1.8047	2.9×10^{5}	8.8
11	0.148±0.006	5.28±0.21	2.0611	2.4×10^{4}	1.9
12	0.058±0.006	2.72±0.55	1.3483	1.4×10^{4}	2.7

* in particles/m^2-sr-s-MeV/nucleon; ** in particles/m^2-sr-MeV/nucleon.

$$Eobs = (\sum_{i} Eobs(i) \quad (2)$$

is the total observed energy deposited in the detectors. DE represents the averaged (with equal weight) relative deviation between calculated and observed energy deposits for the incident particle. (Note: the dead layer in each detector is taken into account in the calculation.) A minimum DE for each good helium candidate is then obtained by employing an iterative technique. It is found that most helium candidates concentrate near charge = 2 and DE < 2.5%. Helium candidates with DE values larger than 2.5% are small in number and are distributed randomly from charge = 1.5 to 2.5. These events are rejected as background in determining the isotopic ratio but are corrected for in the calculation of the absolute flux. For orbit 593, as an example, there is a total of 2054 particles, at L > 6 that satisfy the above three criteria, of which 8 particles have charge larger than 2.5 and 147 particles have charge less than 1.5. A DE < 2.5% cut leaves 1827 out of the 1899 helium counts, so that the ratio of He with DE < 2.5% to total helium is 96.2%.

B. Flux Calculations:

The helium energy spectra is one of the key parameters in analyzing these flares. Table 1 gives the flare parameters along with an intensity (column 6) in the form of the peak helium counts/orbit. For relatively quiet orbits, this rate is 14 counts/orbit. The 12 flares in the Table were selected so that their intensity was an order of magnitude above the quiet-time value. Integrating over the full event, there are sufficient helium particles to measure the energy spectrum.

The CRRES satellite was in a geosynchronous transfer orbit (GTO) and traveled through the magnetosphere from a perigee of ~350 km to an apogee of ~33,580 km with an inclination of 18.2 degrees. Helium with different energies observed at various positions in the orbit (i.e. different L shells) will experience different geomagnetic cutoff effects. The top panel in Figure 2 displays the helium counting rate (normalized for live time) as a function of L shell for orbit 774. Helium above 40 MeV/nucleon can freely access L > 5, in agreement with the transmission function calculations. In addition, most helium is detected at L > 6 (middle panel in Fig. 2) since the spacecraft spends most time at high L shells (bottom panel in Fig. 2). Therefore, the analysis is limited to data with L > 6. Such a choice avoids proton pile-up when the instrument passes through the inner radiation belt as well as geomagnetic transmission effects.

Since the ONR-604 experiment is a range telescope, the geometry factor is a function of the particle energy. This has been calculated for a full model of the telescope and the result is shown in Figure 3. The acceptance peaks at the lowest energies, ~50 MeV/nucleon, and falls off steadily for higher energies.

The measured flux must also be corrected for the Galactic Cosmic Ray (GCR) background. From an analysis of 784 quiet orbits during the CRRES mission, the GCR levels are found to be 5.94 counts per orbit for ID ≥ 7 and 4.11 counts/orbit for ID ≥ 8.

Then, the SEP helium spectrum at L > 6 is obtained by taking into account the instrument efficiency, the DE-cut correction, the geometry factor of the instrument (corresponding to RS < 18.75 mm), and the live time. The live time excludes data gaps, calibration times and rate dead time. A representative ^4He (L > 6) energy spectrum is displayed in Figure 4, which shows the result obtained for SEP event 4 (March 22, 1991). The spectrum follows a fairly straight line, and this feature is representative of the other SEP events as well. Therefore, the spectrum is parametrized by fitting it to a power law form,

$$dJ/dE = A(E/E_0)^{-\gamma}, \quad (3)$$

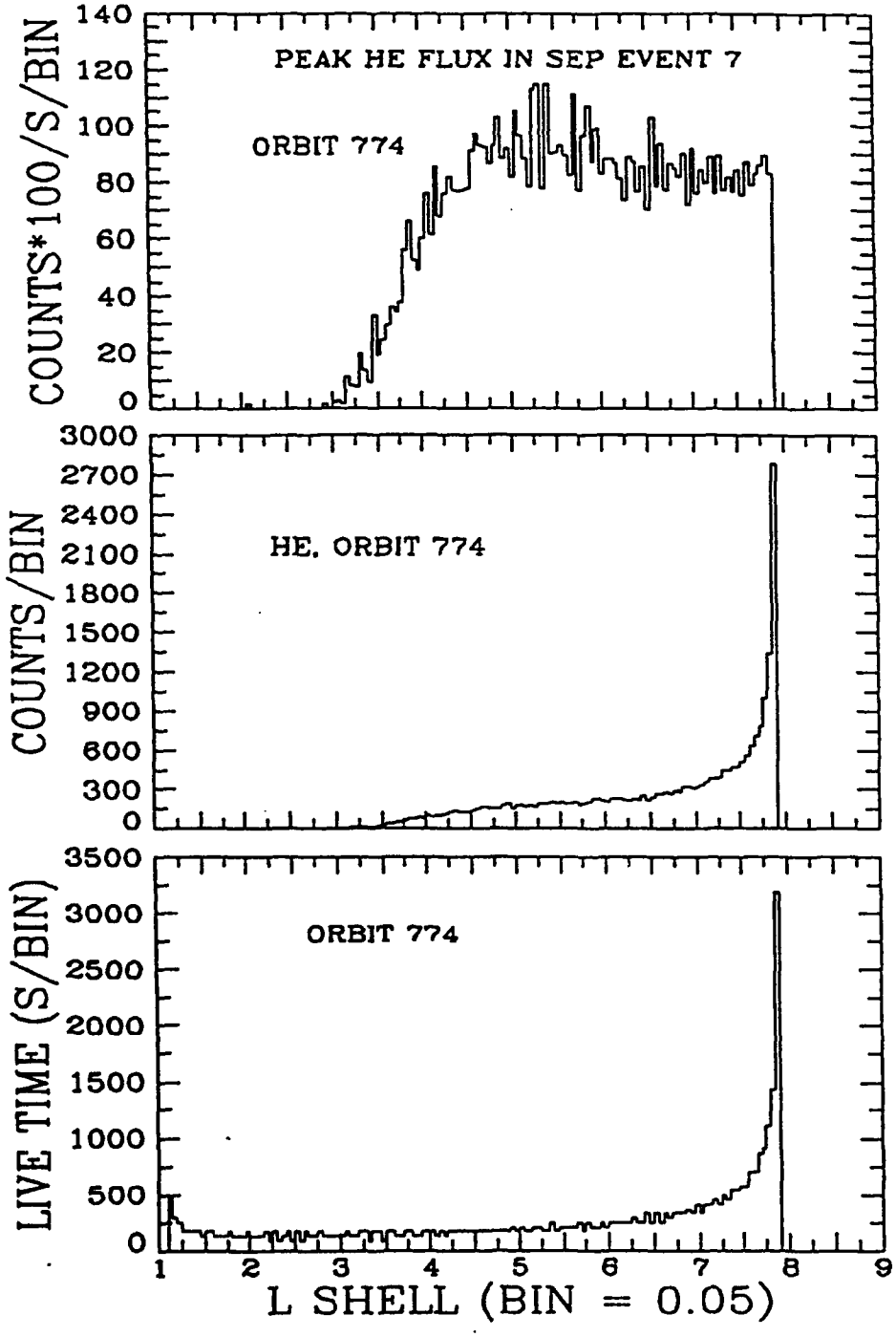

Figure 2. Normalized Helium counting rate for Orbit 774 (top), composed of the raw rate (center) divided by the available observation time (bottom), all as a function of L.

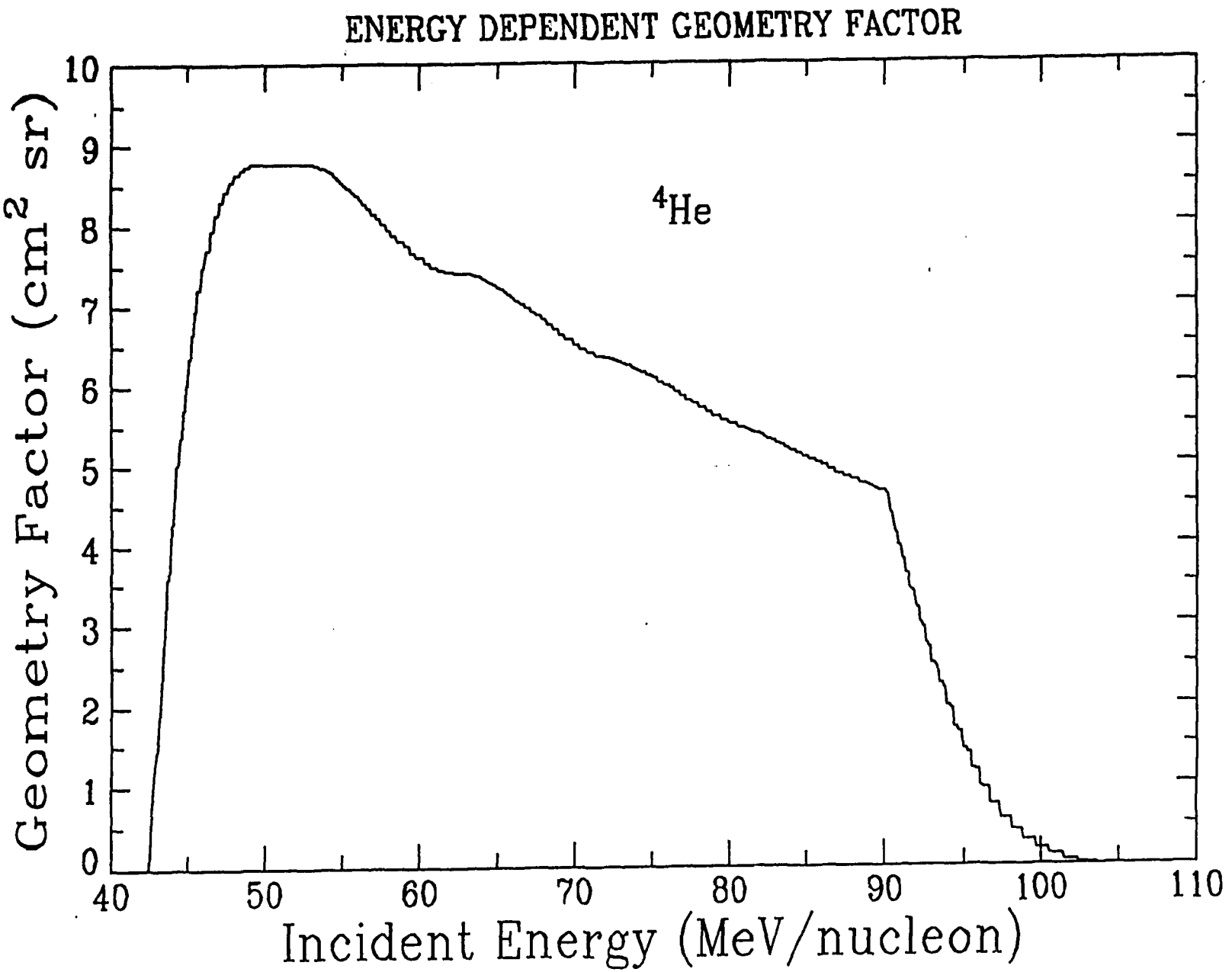

Figure 3. The energy dependence of the geometrical factor for ONR-604 for ^{4}He.

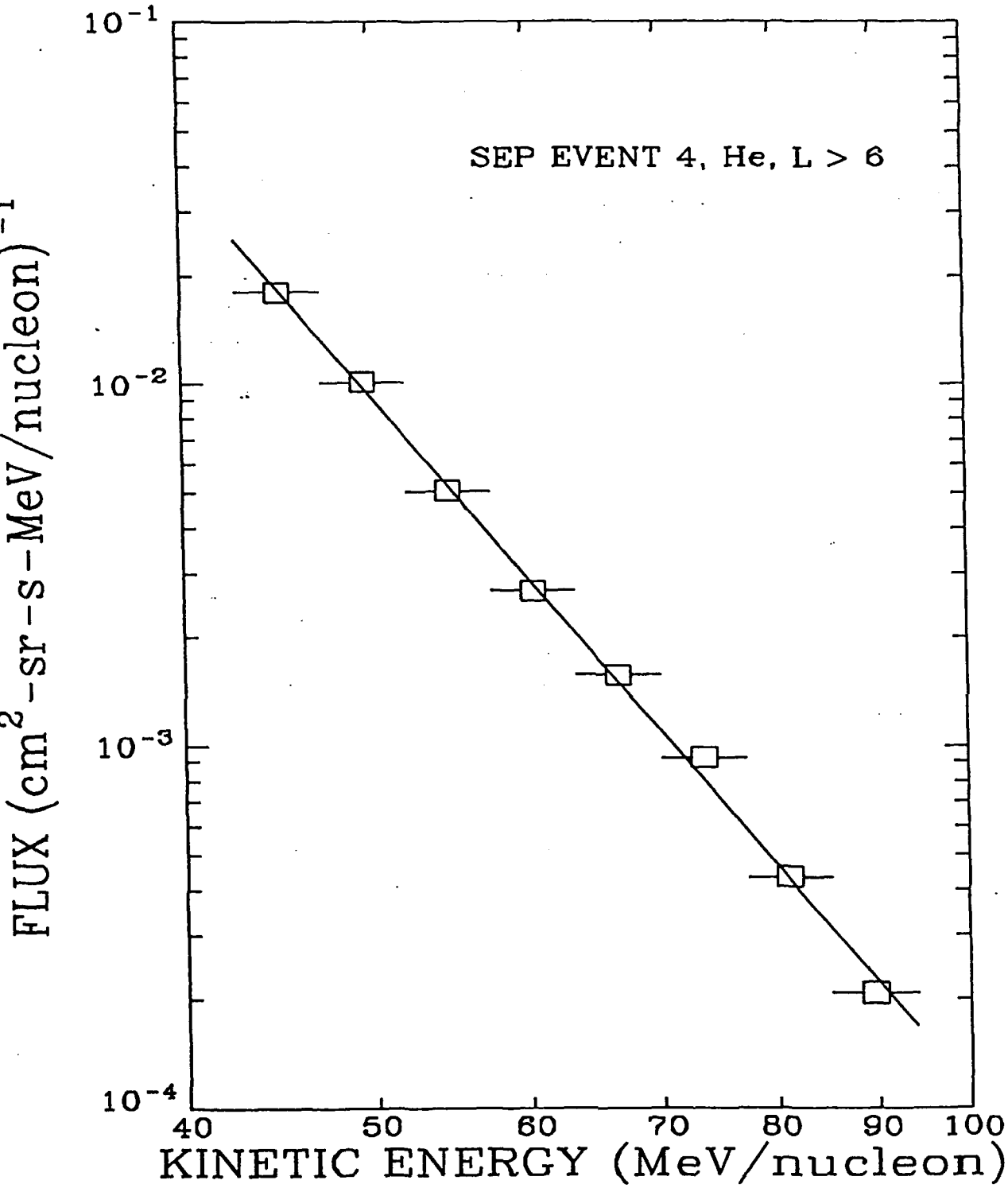

Figure 4: Helium energy spectrum for event number 4, the flare of 22 March, 1991.

where E_0 is a reference energy; A is the amplitude of the spectrum; and γ is the spectral index. In the present analysis, E_0 has been chosen as 66 MeV/nucleon. The solid line in Figure 4 is the least-squares fit which is an excellent representation of the observed data. The fitted spectrum parameters for each of the 12 SEP events are tabulated in Table 2 (A in column 2 and γ in column 3). The estimated error bounds for both spectral index and amplitude are from the uncertainties in the least-squares fitting. It is important to note that the spectral amplitude, in fact, is the average flux at energy E_0. Table 2 also tabulates the duration of each SEP event (column 5) and the average fluence (column 4). The latter is simply the product of the average flux and the duration, which represents the importance of a given SEP event.

The results in Table 2 are interesting since they show a wide variety of spectral indices ranging from hard spectra with $\gamma \approx$ 1-2 to soft spectra with $\gamma \sim$5-6. The fluence column reveals that event 8 is the most prodiguous product of particles with events 4, 7, and 9 not too far behind. Together, these four events dominate the SEP contribution during the CRRES mission.

An initial attempt at validating the solar flare spectra derived from ONR-604 employed the 25-93 MeV/nucleon helium flux from IMP-8 provided by the University of Chicago. A comparison for event 7 is shown in Figure 5, and the agreement is good. However, the size of the IMP-8 energy range covers most of the helium that we measure, and then some. This is not a very precise comparison, but it does indicate that the ONR-604 results are reasonably close. We are currently investigating using the 70-95 MeV/nucleon helium data derived from IMP-8 to give a more precise comparison, and hopefully act as proof of the helium spectrum measurements.

C. Proton Spectra:

The proton events in ONR-604 are located in priority #3 which contains much low-Z background. Consequently, we have used the proton channels from the GOES-7 spacecraft, from the data provided by The National Geophysical Data Center. A least squares fit to a power law for that data is shown in Figure 6 and yields spectral indices of -4.7 ± 0.4 and -3.1 ± 0.2 for the March and June periods, respectively. These are to be compared to the Helium spectra which have peak spectral indices of -6.8 ± 0.2 and -4.3 ± 0.1 for the same flares. Clearly, more precise proton data would be valuable in the SEP analysis.

The comparison of proton and helium spectra are important, since proton spectra have, traditionally, been used to characterize a flare event and to extrapolate to other species. The protons show harder spectra than the helium by a considerable amount. The ratio γ (He)/γ (p) is 1.4 ± 0.1 for both the March and June flares, which are of two different types. It is not clear whether such a ratio is characteristic of all the flares, but this is a parameter to be investigated for the rest of the flares in Table 1.

One of our goals has been to look at the P3 events from ONR-604 to determine if it would be possible to extract proton spectra. What we have discovered is that there are insufficient P3 events in ONR-604 during a flare to provide a measurement of the proton spectrum. In hindsight, this should have been obvious. The P1, P2, P3 priority system was designed to give greatest weight in the pulse height analysis to the heaviest nuclei: P1 over P2 over P3. During a flare there is so much helium, in P2, that the P3 analysis mode gets little or no time. In quiet-times there are many P3 events, but not during intense flare periods. Thus, we will have to look elsewhere for more precise proton data to determine the spectral ratios.

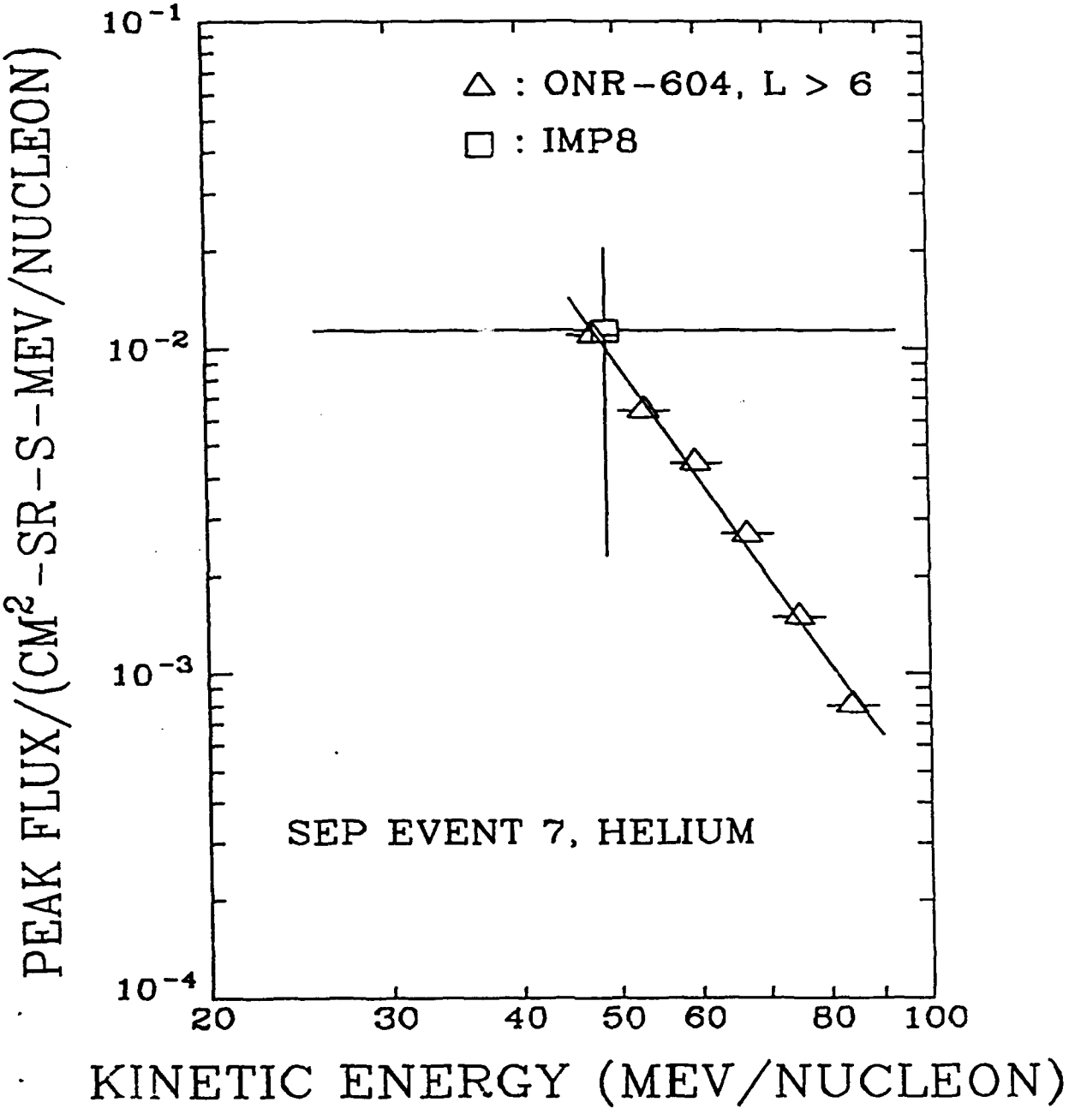

Figure 5: Comparison of the energy spectrum measured by ONR-604 for event 7 with IMP-8 results.

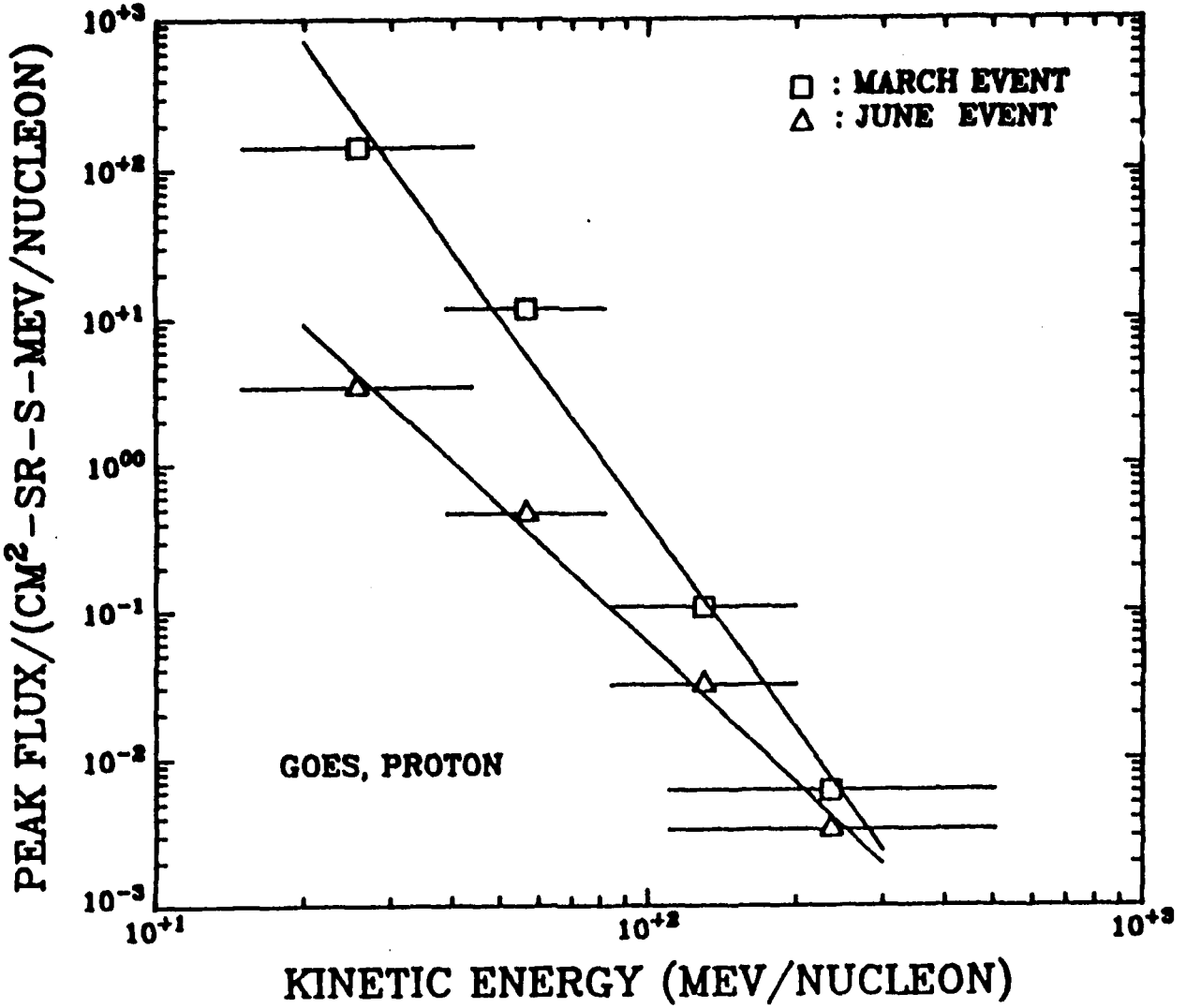

Figure 6: Energy spectra for protons for the March and June 1991 flare periods derived from the GOES-7 data.

D. Isotope Ratios:

It should be noted that the resolution of the ONR-604 instrument is sufficient to separate the isotopes of Helium. One indication of heavy ion enhancement in solar flares has been an accompanying enhancement in the $^3He/^4He$ ratio. We have begun to investigate the use of this ratio, and Figure 7 shows a summary of the preliminary mass histograms for the helium from the different flares. In most of the events the ^3He is barely discernible (as would be expected) and must be extracted from the tail of the ^4He peak. However, in several events, most notably event 5 (24 March 1991), there is sufficient ^3He to define the ratio and to make a spectral measurement.

The preliminary analysis of event 5 is shown in Figure 8, where the spectra for ^3He and ^4He are plotted separately. The spectral indices are very close, as they should be for acceleration from the same particle population. The ^4He has a power law index of -5.1 while the ^3He fit gives -4.7. The difference may be due to the effect of the different Z/A ratios of the two isotopes during the acceleration process. This may be a significant constraint on the acceleration mechanism.

We plan to continue to refine this analysis over the next few months. In particular, we must investigate the origin of the "tail" on the low-mass side of the ^4He peak. If it cannot be completely eliminated, we will have to develop fitting procedures to estimate the contribution of this tail to the ^3He region of the mass histograms. Then the ratios, or upper limits to the $^3He/^4He$ ratios, can be determined. We can then compare the present data to previous results in the literature and to models that have been proposed for the flare acceleration process and for coronal and interplanetary transport of the SEP ions.

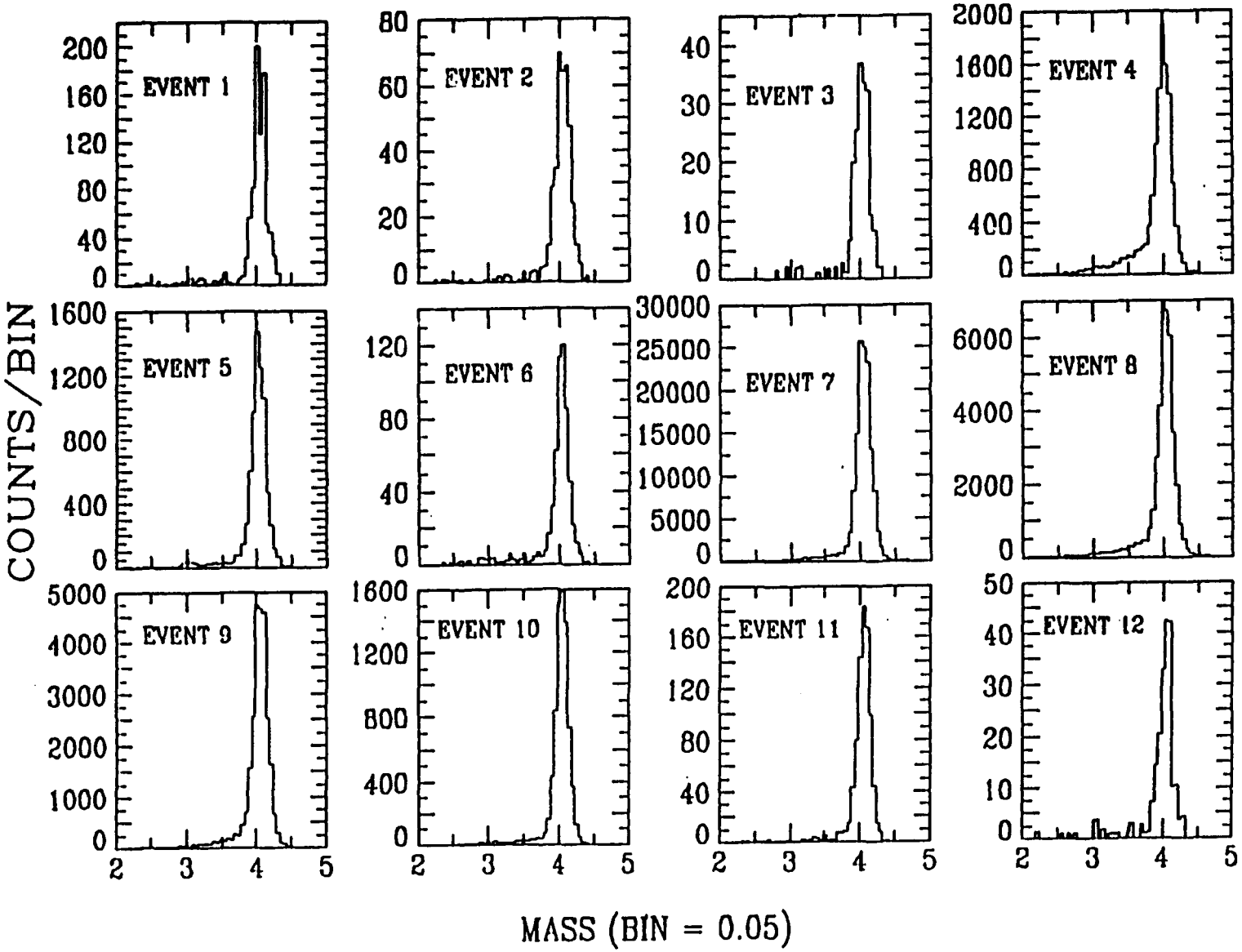

Figure 7: Preliminary Helium mass histograms for each of the twelve SEP events occurring during the CRRES mission that have been identified for study.

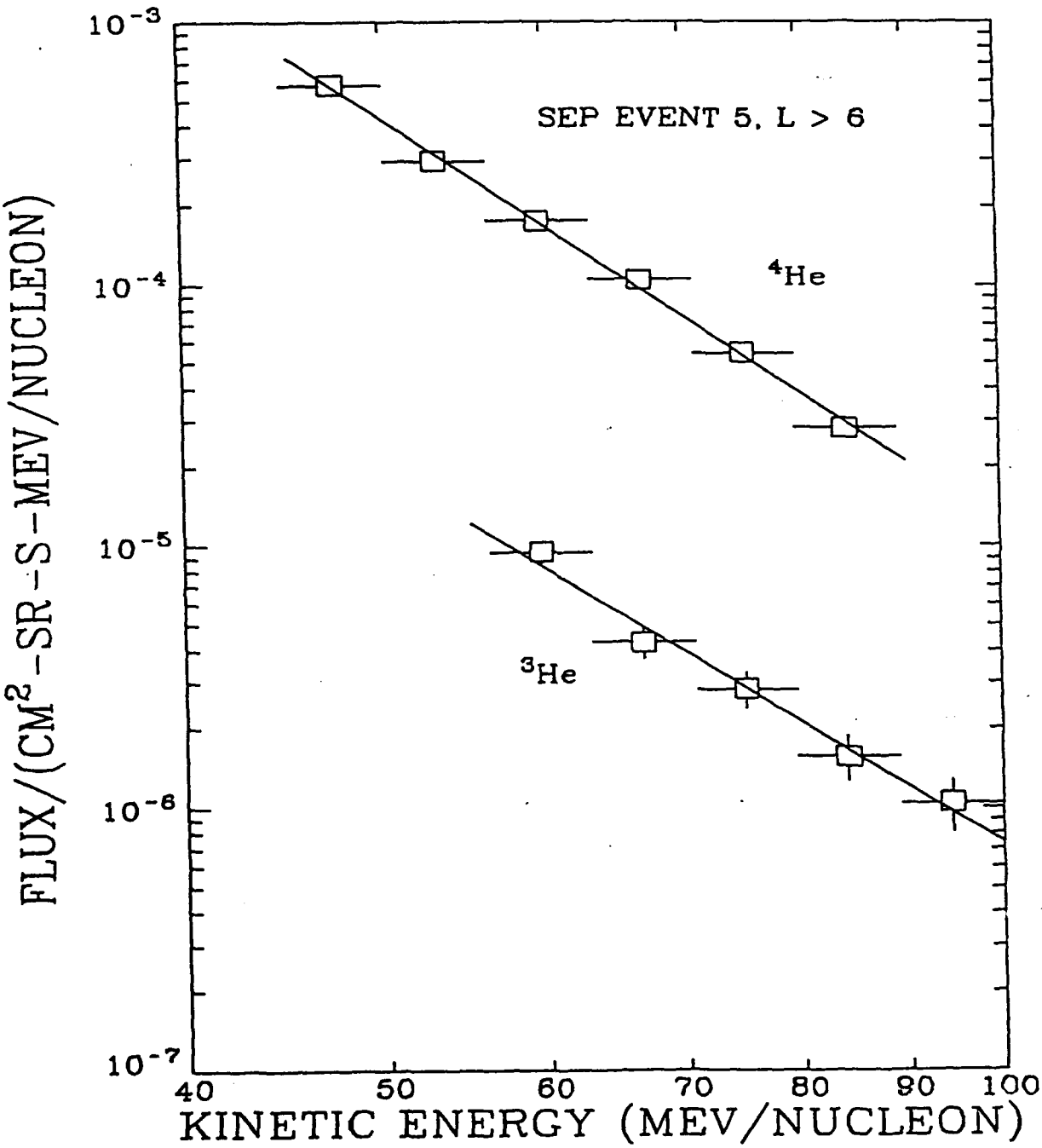

Figure 8: Energy spectra for both ^{4}He and ^{3}He from SEP event 5.